THE JOURNAL OF BIOLOGICAL CHEMISTRY VOL. 289, NO. 28, pp. 19556–19569, July 11, 2014

Syntaxin 8 Modulates the Post-synthetic Trafficking of the TrkA Receptor and Inflammatory Pain Transmission*◆

Received for publication, March 26, 2014, and in revised form, May 8, 2014 Published, JBC Papers in Press, May 28, 2014, DOI 10.1074/jbc.M114.567925

Bing Chen, Ling Zhao, Xian Li, Yun-Song Ji, Na Li, Xu-Feng Xu, and Zhe-Yu Chen[1]

From the Department of Neurobiology, Shandong Provincial Key Laboratory of Mental Disorders, School of Medicine, Shandong University, Number 44 Wenhua Xi Road, Jinan, Shandong 250012, China

Background: Proper cell surface location of TrkA is crucial for NGF-mediated functions; however, the mechanisms modulating TrkA surface levels remain unclear.
Results: Syntaxin 8 increases TrkA surface levels and modulates inflammatory pain transmission.
Conclusion: Syntaxin 8-regulated TrkA surface targeting is essential for NGF-mediated functions.
Significance: These findings advance our understanding of the mechanisms of TrkA surface targeting and pain transmission.

Nerve growth factor (NGF) promotes the survival, maintenance, and neurite outgrowth of sensory and sympathetic neurons, and the effects are mediated by TrkA receptor signaling. Thus, the cell surface location of the TrkA receptor is crucial for NGF-mediated functions. However, the regulatory mechanism underlying TrkA cell surface levels remains incompletely understood. In this study, we identified syntaxin 8 (STX8), a Q-SNARE protein, as a novel TrkA-binding protein. Overexpression and knockdown studies showed that STX8 facilitates TrkA transport from the Golgi to the plasma membrane and regulates the surface levels of TrkA but not TrkB receptors. Furthermore, STX8 modulates downstream NGF-induced TrkA signaling and, consequently, the survival of NGF-dependent dorsal root ganglia neurons. Finally, knockdown of STX8 in rat dorsal root ganglia by recombinant adeno-associated virus serotype 6-mediated RNA interference led to analgesic effects on formalin-induced inflammatory pain. These findings demonstrate that STX8 is a modulator of TrkA cell surface levels and biological functions.

Neurotrophins are important regulators of neural survival, development, synapse formation, and synaptic plasticity (1, 2). Nerve growth factor (NGF) was the first neurotrophin identified, and it plays pivotal roles in both embryonic development and the adult functions of certain target neurons, especially in the peripheral nervous system (3). NGF signaling occurs through two distinct receptors, $p75^{NTR}$ and TrkA. Although $p75^{NTR}$ binds to all neurotrophins with similar affinities, TrkA receptors display selectivity toward NGF (4, 5). NGF binds the extracellular domain of TrkA, initiating receptor phosphorylation and activating downstream signal transduction cascades, including the Ras/mitogen-activated protein kinase (MAPK) and PI3K/protein kinase B (Akt) pathways (6). Therefore, NGF-mediated signal transduction and biological functions appear to be determined at least partially by the levels of TrkA receptors at the plasma membrane. The cell surface levels of TrkA depend on two opposite processes as follows: newly synthesized TrkA receptor insertion into the plasma membrane and TrkA endocytosis from the cell membrane. The removal of TrkA receptors from the plasma membrane by endocytosis has been studied in detail (7–9). However, the mechanism underlying the insertion of newly synthesized TrkA receptors into the plasma membrane is less well understood.

To uncover novel TrkA-interacting proteins and learn more about the mechanisms that modulate TrkA surface localization, a yeast two-hybrid assay was performed, and it identified several candidate TrkA-associated proteins, one of which was syntaxin 8 (STX8). STX8 is a member of the Q-SNARE family (Q-soluble *N*-ethylmaleimide-sensitive factor attachment protein receptor), and Q-SNAREs mediate membrane fusion through interactions with their cognate R-SNARE partners to form organelle-specific docking and fusion complexes in eukaryotic cells (10, 11). Syntaxins as Q-SNARE members interact with a wide range of receptors and dynamically regulate their trafficking (*i.e.* insertion, internalization, recycling, and degradation). For example, syntaxin 16 mediates recycling of the cyclic AMP-dependent chloride (cystic fibrosis transmembrane conductance regulator) channels and regulates their surface levels in polarized epithelial cells (12). Syntaxin 6 affects the Golgi-related transport and cell surface levels of vascular endothelial growth factor receptor 2 (VEGFR2) (13). A recent study suggested that STX8 regulates cystic fibrosis transmembrane conductance regulator channels trafficking and its chloride transport activity (14).

In light of the interaction between STX8 and TrkA and the annotation of STX8 as a member of the protein-trafficking Q-SNARE family, we addressed the possibility that STX8 might regulate TrkA intracellular trafficking. Our study showed that STX8 regulates TrkA cell surface levels by promoting TrkA trafficking from the Golgi to the plasma membrane.

* This work was supported by National 973 Basic Research Program of China Grants 2012CB911000 and 2010CB912004, National Natural Science Foundation of China Grants 31130026 and 31101027, the State Program of National Natural Science Foundation of China for Innovative Research Group Grant 81321061, and the Foundation for Excellent Young Scientist of Shandong Province Grant BS2010SW023.
◆ This article was selected as a Paper of the Week.
[1] To whom correspondence should be addressed. Tel.: 86-531-88382336; Fax: 86-531-88382329; E-mail: zheyuchen@sdu.edu.cn.

EXPERIMENTAL PROCEDURES

Reagents and Antibodies—Murine recombinant NGF was purchased from Harlan Bioproducts for Science (Indianapolis, IN). Rabbit anti-TrkA and anti-TrkB antibodies were from Millipore (Temecula, CA); polyclonal anti-Trk (C-14) antibody was from Santa Cruz Biotechnology (Santa Cruz, CA); mouse anti-STX8 antibody was from BD Biosciences Pharmingen (San Jose, CA); mouse anti-FLAG, anti-Akt, anti-tubulin, and rabbit anti-HA antibodies were from Sigma; rabbit anti-phospho-TrkAY490, anti-ERK1/2, anti-phospho-AktS473, and mouse anti-phospho-ERK1/2 were from Cell Signaling Technology (Beverly, MA); rabbit anti-active caspase-3 antibody was from Abcam (Cambridge, MA). Horseradish peroxidase (HRP)-conjugated goat anti-mouse and anti-rabbit IgG were from Calbiochem; Alexa Fluor-488- or 594-conjugated goat anti-mouse or anti-rabbit IgG (H+L) were from Invitrogen. The restriction enzymes were from MBI Fermentas (Hanover, MD), and sulfo-NHS-biotin and sulfo-NHS-S-S-biotin were purchased from Pierce. All cell culture reagents were from Invitrogen. The other reagents were obtained from Sigma.

Plasmid Constructs—The coding region of rat full-length TrkA or TrkB cDNAs with an N-terminal FLAG epitope tag added after the signal peptides by PCR were subcloned into the pEGFP-N1 and pCDNA3.1 expression vectors (Invitrogen), respectively. Full-length STX8 cDNA with a C-terminal HA epitope tag was cloned into the pCDNA3.1 and pmRFP-N1 expression vectors. All the TrkA STX8 deletion constructs and the TrkA TrkB chimeric constructs were generated by two-step PCRs. To knock down the expression of STX8, 19 nucleotides (5′-GACAGAACCTTCTGGATGA-3′) were targeted with siRNA using the pSuper expression vector (OligoEngine, Seattle, WA) with the red fluorescent protein (RFP)[2] sequence. The sequences of all of the constructs were confirmed by DNA sequencing.

Cell Lines and Dorsal Root Ganglia (DRG) Neuron Cultures—Human embryonic kidney cell line 293 (HEK293) cells were grown in Dulbecco's modified Eagle's medium (DMEM) containing 10% fetal bovine serum (FBS) supplemented with 100 units/ml penicillin/streptomycin and 2 mM L-glutamine. Rat pheochromocytoma cell line 12 (PC12) cells were maintained in DMEM containing 5% FBS, 10% horse serum supplemented with 100 units/ml penicillin/streptomycin, and 2 mM L-glutamine. The 615 cell line was PC12 cells stably expressing the TrkA receptor cultured as described previously (15). DRG neurons were dissected from embryonic day 18 (E18) Wistar rats and grown in Neurobasal medium containing 2% B27 supplement (Invitrogen), 0.5 mM L-glutamine, 100 units/ml penicillin/streptomycin, and 50 ng/ml NGF at 37 °C, 5% CO_2, and 95% humidity. Proliferating cells disappeared after 3–4 days of incubation with arabinofuranosyl cytidine, and more than 95% of the cells at 4 days *in vitro* were neurons.

Surface Biotinylation and Western Blot Analysis—Cell surface receptor biotinylation was performed in 615 cells as described previously (16). Briefly, 615 cells were transfected with the indicated cDNAs by electroporation. 48 h later, serum-starved cells were washed twice with ice-cold phosphate-buffered saline (PBS) at pH 7.4 supplemented with 0.1 mM Ca^{2+} and 1 mM Mg^{2+} and then incubated with 300 μg/ml sulfo-NHS-biotin in PBS to biotinylate surface proteins for 45 min at 4 °C. Unreacted biotin was washed out with Tris-buffered saline (TBS). The cells were immediately lysed and precipitated with 20 μl of immunopure immobilized streptavidin (Pierce) at 4 °C overnight. Washed beads were eluted with SDS sample buffer, and eluted proteins were separated by SDS-PAGE and then blotted with a polyclonal anti-Trk (C-14) antibody. Immunoreactive bands were quantified using ImageJ (Scion, Frederick, MD).

For the cleavable surface biotinylation assay, surface receptors were biotinylated with sulfo-NHS-S-S-biotin at 4 °C. After NGF treatment for 15 min, the internalization was terminated by washing with ice-cold TBS, and the remaining cell surface biotin was stripped with glutathione (17). Then the cells were lysed, and the biotinylated proteins were precipitated with streptavidin beads and subjected to Western blotting.

PC12 Cell Fractionation Analysis—PC12 cells (80–100 million) were collected by digesting with 0.25% trypsin and washed once with 1 mM EDTA in PBS and then with sucrose buffer (250 mM sucrose, 10 mM triethylamine, pH 7.4, and 1 mM EDTA). Next, the cells were homogenized on ice using ~30 strokes of a glass Dounce homogenizer in 0.5 ml of buffer (320 mM sucrose, 10 mM Hepes, pH 7.2, with protease inhibitors) and centrifuged at 500 × *g* for 2 min. The post-nuclear supernatant was then subjected to fractionation by centrifugation at 105,000 × *g* for 120 min in an SW60 Ti rotor (Beckman Instruments) and layered on a discontinuous sucrose density gradient (15, 30, 40, and 55%). Fractions of 0.4 ml were collected from the top (designated fraction number 1 (top) to 13 (bottom)). An aliquot of each fraction (50 μl) was mixed with protein sample buffer and assayed by immunoblotting.

Immunocytochemical Staining and Microscopic Quantitative Analysis—Ratiometric fluorescence assays to measure the levels of the Trk receptors in the plasma membrane were performed as described previously (18). In brief, PC12 cells were transfected with FLAG-Trk-GFP and STX8-HA in a 1:3 ratio using Lipofectamine 2000 (Invitrogen). 24 h later, the cells were fixed with 4% paraformaldehyde and stained with an anti-FLAG M2 monoclonal antibody under nonpermeabilizing conditions and then with an Alexa Fluor-594-conjugated goat anti-mouse secondary antibody (1:500; Invitrogen). Fluorescence images were acquired by a Nikon Eclipse TE 2000-U microscope, and the confocal fluorescence images were collected using a Zeiss LSM780 confocal microscope (Microstructural Platform of Shandong University). All of the images were collected by a 60 × objective lens, and a quantitative analysis was carried out with MetaMorph software (Universal Imaging Corp., West Chester, PA). Relative surface receptor levels were

[2] The abbreviations used are: RFP, red fluorescent protein; TGN, trans-Golgi network; DRG, dorsal root ganglia; rAAV, recombinant adeno-associated virus serotype; ER, endoplasmic reticulum; CT, C-terminal; ANOVA, analysis of variance; RFP, red fluorescent protein; IP, immunoprecipitation; CC, correlation coefficient.

defined as the ratios of surface Alexa Fluor-594/total GFP fluorescence intensity.

Ratiometric fluorescence assays were performed to measure the internalization of FLAG-TrkA from the cell surface. After serum starvation for 12 h, PC12 cells transfected with FLAG-TrkA and other indicated cDNAs were incubated with the calcium-sensitive anti-FLAG antibody M1, which was conjugated to Alexa Fluor-488 for 1 h at 4 °C. Then 50 ng/ml NGF was added for 15 min at 37 °C to drive receptor internalization. After NGF incubation, cells were fixed with 4% paraformaldehyde and stained with Cy5-conjugated anti-mouse secondary antibody to label receptors that remained at the cell surface. Therefore, Alexa Fluor-488 M1-labeled FLAG-TrkA includes the internalized and the remaining TrkA at the cell surface, whereas Cy5-labeled FLAG-TrkA represents the remaining surface receptor. The staining intensity for each of the selected cells was measured by MetaMorph software. Meanwhile, cells without NGF incubation were used as a parallel control (100% surface control). The percentage of TrkA internalization was calculated from the Cy5/488 intensity ratio determined in the control condition according to the following formula: $(1 - E/C) \times 100\%$, where E is the mean ratio for internalized group, and C is the mean ratio for 100% surface control group.

Immunohistochemistry—DRG (L4 and L5) were removed from adult rats, post-fixed at 4 °C overnight, and cryoprotected in a 30% sucrose solution (in 0.01 M PBS, pH 7.4) at 4 °C for 72 h. DRG were embedded in cryoembedding fluid, sectioned at 14-μm thickness, and mounted directly onto slides. The sections were washed in PBS, and citrate-based "antigen retrieval" was performed. Briefly, the slides were heated in citrate buffer (0.1 M citrate buffer: 0.1 M sodium citrate buffer = 1:4.6) and maintained at 92–98 °C for 10 min. The sections were then cooled for 20 min and incubated with primary antibodies (rabbit anti-TrkA and mouse anti-STX8) at 4 °C overnight after nonspecific binding was blocked by incubation in 3% normal goat serum in PBS with 0.3% Triton X-100 for 3 h. After three washes in PBS, the sections were incubated with corresponding secondary antibodies.

Lentiviral Supernatant Preparation and Cell Lentiviral Transduction—The STX8 and STX8ΔTM (1–648 bp) sequences followed by RFP sequence were cloned into the bidirectional pCCL lentiviral vector to produce pCCL-STX8 RFP and pCCL-STX8ΔTM RFP. pCCL-RFP was used as a control construct. The lentiviruses were produced by transient transfection of HEK293T cells using Lipofectamine 2000 with the pCCL constructs as well as with pMDLg/pRRE, pRSV-Rev, and pMDG-VSVG. After 48 h, the supernatant containing the lentivirus was collected and filtered through a 0.45-μm filter. A total of 200 μl of supernatant containing the lentivirus was added to the medium to transfect 1×10^5 DRG neurons.

Animals, Vector Delivery, and the Formalin Test—All animal procedures were carried out with approval from the National Institutes of Health Guide for the Care and Use of Laboratory Animals and the Institutional Animal Care and Use Committee of Shandong University. Male Wistar rats (200–250 g) were housed under 12-h light/dark cycles with free access to food and water. The rAAV6 and rAAV8 vectors were produced by triple-plasmid transfection of 293T cells. rAAV6-siSTX8-ZsGreen and rAAV8-siSTX8-GFP were prepared at concentrations of 3×10^{12} and 5×10^{12} vector genomes/ml respectively. A total of $\sim 1.5 \times 10^{11}$ viruses were delivered into the cerebrospinal fluid through lumbar intrathecal injection through the L4/5 intervertebral space. After 4 weeks, immunohistochemistry of the DRG sections and animal formalin tests were performed. For the formalin tests, the rats were first habituated in the observation cages for 30 min. Then 50 μl of a 5% formalin solution was subcutaneously injected into the right hind paw of each rat. The rats were then placed into a testing chamber with a plastic floor to allow an unobstructed view of the paws, and the licking activity was recorded for 60 min after injection on a videotape. The cumulative licking time was calculated and analyzed.

Statistical Analysis—Statistical significance was assessed using Student's *t* test or one-way analysis of variance (ANOVA) followed by post hoc tests. The data are presented as means ± S.E., and a value of $p < 0.05$ was considered significant.

RESULTS

STX8 Associates with TrkA but Not TrkB Receptors—We demonstrated that STX8 associates with TrkA receptors in a yeast two-hybrid assay by screening a rat DRG cDNA library using the intracellular domain of TrkA (amino acids 443–799) as the bait. A physical interaction between STX8 and TrkA was assessed by a co-immunoprecipitation (co-IP) assay in co-transfected HEK293 cells. STX8-HA was clearly detected in FLAG-TrkA immunoprecipitates but not in IP complexes of FLAG-TrkB, even though TrkA and TrkB are homologous (Fig. 1*A*), indicating that the association between STX8 and TrkA was specific. To examine whether this interaction could occur under physiological conditions and exclude the influence of protein overexpression, we performed endogenous co-IP assays with homogenates from DRG, which endogenously express TrkA, TrkB, and STX8. As shown in Fig. 1*B*, endogenous TrkA but not TrkB receptors co-immunoprecipitated with STX8.

Given that TrkA is selectively expressed in small- and medium-sized nociceptive DRG neurons (19, 20), an immunohistochemical analysis was carried out to determine whether TrkA and STX8 are co-expressed in DRG neurons. As shown in Fig. 1*C*, all neurons with TrkA-positive staining also expressed STX8. Furthermore, in cultured DRG neurons, punctate staining of STX8 was found to be co-localized with TrkA (*arrows* in Fig. 1*D*), thus supporting the co-IP analysis of the TrkA/STX8 association. Taken together, these data indicate that STX8 interacts with TrkA receptors in DRG neurons, and the interaction is specific to TrkA but not TrkB.

STX8 Regulates the Surface Levels of TrkA but Not TrkB Receptors—Because STX8, a member of the Q-SNARE subfamily, mediates the sorting and trafficking of cargo proteins (10), we questioned whether STX8 modulates the cell surface levels of TrkA receptors. Thus, gain-of-function and loss-of-function analyses were used to determine the effect of STX8 on cell surface levels of TrkA and TrkB. We first constructed FLAG-Trk-GFP receptors with a FLAG epitope at the extracellular N terminus and a green fluorescent protein (GFP) tag at the intracellular C terminus. The GFP had no effect on the

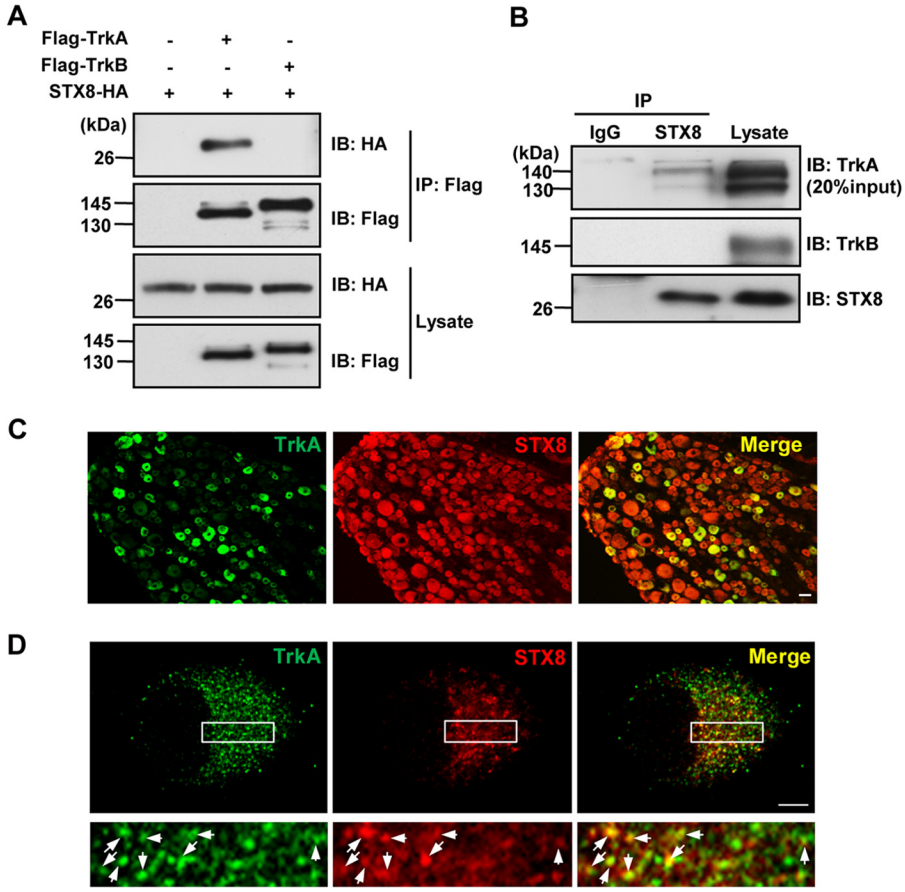

FIGURE 1. **STX8 physically interacts with TrkA but not TrkB receptors.** *A,* co-immunoprecipitation of STX8-HA with FLAG-Trk receptors. Lysates from HEK293 cells transfected with STX8-HA and FLAG-TrkA/TrkB constructs were immunoprecipitated with anti-FLAG antibody. Immunoblotting (*IB*) analysis was performed to detect immunoprecipitated proteins. *B,* endogenous association of STX8 and Trk receptors. Tissue homogenates from adult rat DRG were immunoprecipitated with the STX8 antibody and immunoblotted with Trk antibodies. *C,* immunohistochemical analysis was performed with DRG sections labeled with anti-TrkA (*green*) and anti-STX8 (*red*) antibodies. *Scale bar,* 20 μm. *D,* co-localization of endogenous TrkA and STX8 in cultured DRG neurons visualized by confocal microscopy. The *lower panels* show enlarged images of the *framed regions*. The *arrows* in the combined image indicate punctate staining of co-localized TrkA and STX8. *Scale bar,* 5 μm.

TrkA/STX8 association (Fig. 2*A*). A ratiometric fluorescence assay was performed as described previously (18) to measure the surface levels of Trk receptors. The GFP fluorescence represented the total Trk amount, and the surface Trk was labeled with an anti-FLAG antibody under nonpermeabilizing conditions in transfected PC12 cells. Cell surface receptors were quantified by the fluorescence intensity of FLAG staining normalized to GFP intensity per cell to eliminate the effect of differential receptor expression levels. We observed that STX8 did not alter the total expression of TrkA; however, STX8 overexpression significantly increased the cell surface levels of TrkA but not TrkB receptors (Fig. 2, *B* and *C*). Conversely, introducing STX8ΔTM, which lacks the hydrophobic transmembrane anchor as a dominant-negative form, significantly decreased the surface levels of TrkA but not TrkB receptors (Fig. 2, *B* and *C*). The regulation of Trk cell surface levels by STX8 was consistent with the association of STX8 with the Trk receptors. DRG neurons express both TrkA and STX8 at high levels (Fig. 1), so next we performed the ratiometric fluorescence assay to measure the surface levels of Trk receptors in cultured DRG neurons to confirm the result acquired in PC12 cells. We found that STX8 overexpression resulted in a 1.27 ± 0.11-fold increase, and STX8 inhibition caused a 0.74 ± 0.06-fold reduction of the cell surface TrkA levels, although the cell surface TrkB levels remained unaffected (Fig. 2, *D* and *E*), confirming the regulation of TrkA surface levels by STX8 in cultured DRG neurons.

These regulations were further complemented by the use of an siRNA-mediated expression silencing approach in PC12 cells. As shown in Fig. 2*F*, siSTX8 transfection efficiently knocked down endogenous STX8 expression but had no effect on the expression of an "siRNA-resistant" construct (rSTX8-HA) in PC12 cells. STX8 depletion by siRNA resulted in a reduction in TrkA cell surface levels according to the result of a ratiometric fluorescence assay, and this reduction could be rescued by rSTX8-HA (Fig. 2*G*). In contrast, siSTX8-mediated knockdown had no effect on the TrkB cell surface levels. A surface biotinylation assay was employed in PC12 cells that stably overexpressed TrkA (615 cells) and confirmed our previous quantitative fluorescence results that STX8 overexpression increased while its inhibition decreased the cell surface levels of the TrkA receptors (Fig. 2*H*). The surface biotinylation assay was also performed under endogenous TrkA expression conditions in DRG neurons. We first generated lentivirus harboring STX8-RFP, STX8ΔTM-RFP, or control

RFP and infected DRG neurons with these lentiviruses to overcome the drawback of low transfection efficiency. Statistical analysis of the biotinylation assay yielded a similar result as that in 615 cells; STX8 overexpression positively regulated the cell surface levels of TrkA, although STX8ΔTM had the opposite effect (Fig. 2*I*). These results suggested that STX8 specifically regulates TrkA but not TrkB cell surface levels in both PC12 cells and DRG neurons.

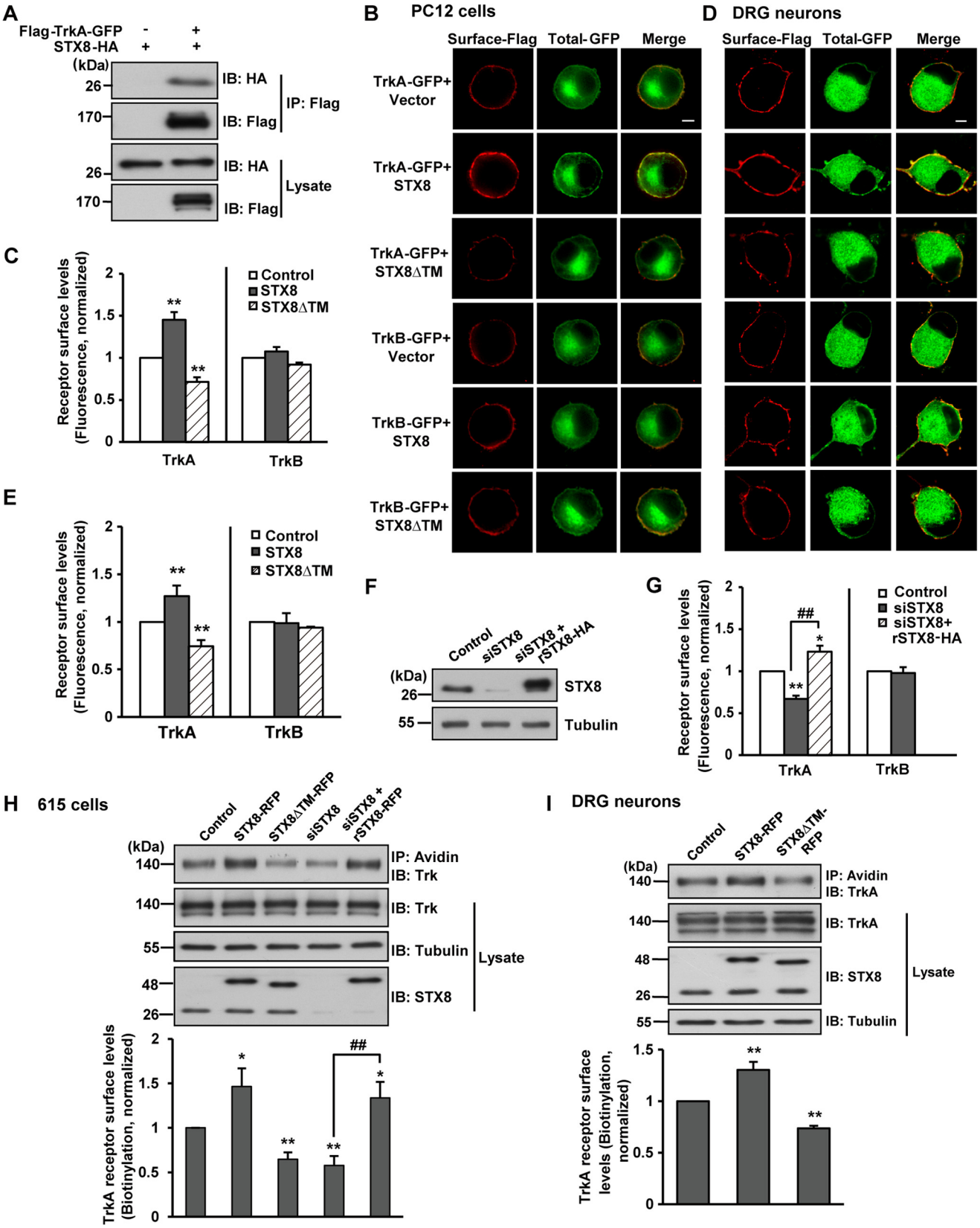

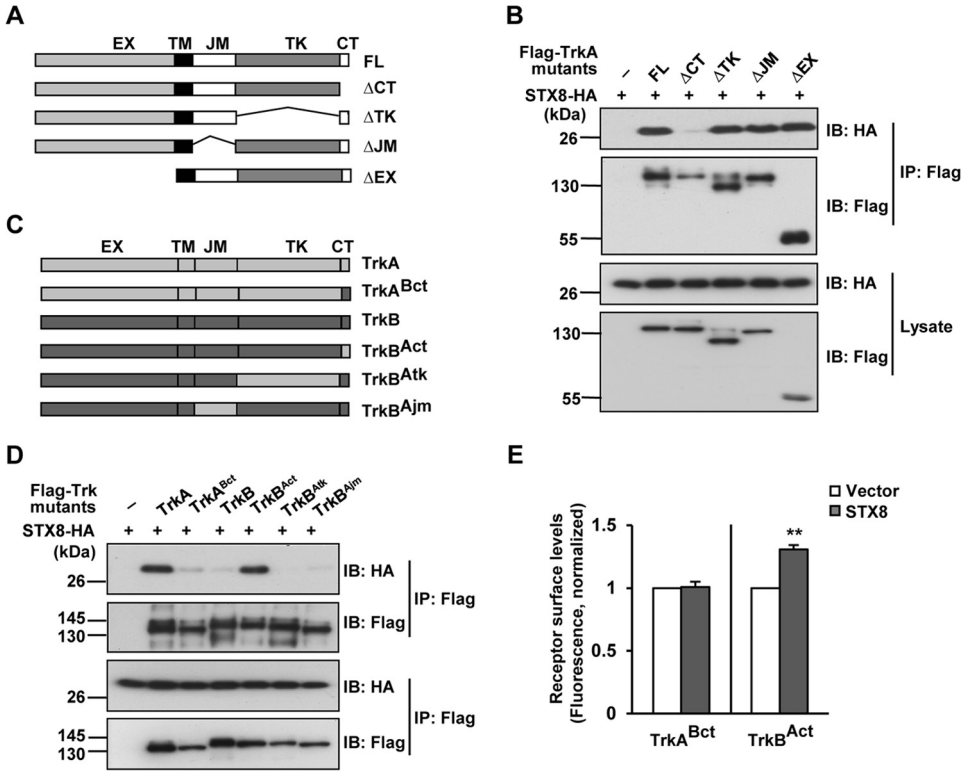

FIGURE 3. **STX8 regulates TrkA cell surface levels by interacting with the TrkA CT domain.** *A,* schematic representation of the TrkA-truncated mutants. *FL,* full-length domain; *CT,* C-terminal domain; *TK,* kinase domain; *JM,* juxtamembrane domain; *EX,* extracellular domain. *B,* co-immunoprecipitation of STX8-HA with FLAG-tagged TrkA truncated mutants. Lysates from transfected HEK293 cells were immunoprecipitated with anti-FLAG antibody followed by immunoblotting (*IB*) with HA and FLAG antibodies. *C,* schematic representation of chimeric TrkA or TrkB receptors with domain substitutions. *D,* co-immunoprecipitation of STX8-HA and FLAG-tagged Trk chimeras in HEK293 cells. *E,* quantification of the surface levels of $TrkA^{Bct}$ or $TrkB^{Act}$ chimeric receptors by the ratiometric fluorescence assay in PC12 cells co-transfected with STX8-HA. The data were normalized to their respective controls and are shown as means ± S.E. from at least three independent experiments (**, $p < 0.01$, Student's *t* test).

TrkA C Terminus Is Necessary and Sufficient for the TrkA/STX8 Interaction—To identify the domain of the TrkA receptor responsible for the STX8 association, we generated a series of mutants (TrkAΔCT, TrkAΔTK, TrkAΔJM, and TrkAΔEX) in which various domains were deleted from full-length TrkA as follows: the C-terminal domain (CT), kinase domain (TK), juxtamembrane domain (JM), and extracellular domain (EX), respectively. The co-IP assay in HEK293 cells indicated that STX8 was detected in the IP complexes of all TrkA-deleted mutants except for TrkAΔCT, which carried the CT (amino acids 786–800) deletion, suggesting that STX8 may interact with the TrkA CT (Fig. 3, *A* and *B*). To confirm this result, we replaced the CT region of TrkB with that of TrkA to generate the $TrkB^{Act}$ chimera, and we observed that this protein significantly associated with STX8 (Fig. 3, *C* and *D*). In contrast, the $TrkA^{Bct}$ mutant, which consisted of the CT domain of TrkB replacing that of TrkA, lost the interaction with STX8 (Fig. 3, *C* and *D*). These observations suggested that the CT domain is necessary and sufficient for TrkA to interact with STX8. We further investigated whether STX8 regulates the surface levels of the Trk chimeras. By the ratiometric fluorescence assay, we observed that STX8 overexpression increased the surface levels of the $TrkB^{Act}$ but not the $TrkA^{Bct}$ chimera in transfected PC12 cells (Fig. 3*E*), which sug-

FIGURE 2. **STX8 regulates cell surface levels of TrkA but not TrkB receptors in PC12 cells.** *A,* co-immunoprecipitation of FLAG-TrkA-GFP and STX8-HA in HEK293 cells. Lysates were immunoprecipitated with anti-FLAG antibody followed by immunoblotting (*IB*) with anti-FLAG or anti-HA antibodies. *B*, ratiometric fluorescence assay to quantify Trk receptors cell surface levels. PC12 cells transfected with FLAG-Trk-GFP, STX8-HA, STX8ΔTM, or control vector construct were stained with an anti-FLAG antibody under a nonpermeabilization condition to label surface Trk receptors; the GFP fluorescence represented total receptor levels. *Scale bar,* 5 μm. *C,* quantification of Trk surface levels by the ratio of red to green fluorescence intensity in *B* (**, $p < 0.01$, *versus* the respective controls; one-way ANOVA). *D,* ratiometric fluorescence assay to quantify Trk receptors cell surface levels in cultured DRG neurons. The neurons transfected by electroporation with indicated constructs were stained with an anti-FLAG antibody under a nonpermeabilization condition to label surface Trk receptors; the GFP fluorescence represented total receptor levels. The neurons were visualized by confocal microscopy. *Scale bar,* 5 μm. *E,* quantification of Trk cell surface levels by the ratio of red to green fluorescence intensity in *C*. The data were normalized to their respective controls (**, $p < 0.01$, one-way ANOVA). *F,* PC12 cells transfected with siSTX8 or siSTX8 with the siRNA-resistant rSTX8-HA were lysed and immunoblotted with STX8 antibody to detect the STX8-knockdown efficiency by siSTX8. *G,* quantification of surface Trk levels in PC12 cells by the ratiometric fluorescence assay as performed in *B* (*, $p < 0.05$; **, $p < 0.01$, *versus* the control group; ##, $p < 0.01$, *versus* the STX8 knockdown group, one-way ANOVA for TrkA, Student's *t* test for TrkB). *H,* cell surface levels of TrkA receptors were evaluated by surface biotinylation assay in 615 cells (PC12 cells stably expressing TrkA) transfected by electroporation. *Lower panel*, quantification of the surface levels of TrkA receptors by the ratio of surface to total TrkA intensity normalized to the control group. All of the data are shown as means ± S.E. from at least three independent experiments (*, $p < 0.05$; **, $p < 0.01$, *versus* the control group; ##, $p < 0.01$, *versus* the STX8 knockdown group, one-way ANOVA). *I,* TrkA cell surface levels were measured by surface biotinylation assay in cultured DRG neurons infected with lentiviruses harboring STX8-RFP, STX8ΔTM-RFP, or control RFP. *Lower panel*, quantification of TrkA cell surface levels. All of the data are shown as means ± S.E. from at least three independent experiments (**, $p < 0.01$, one-way ANOVA).

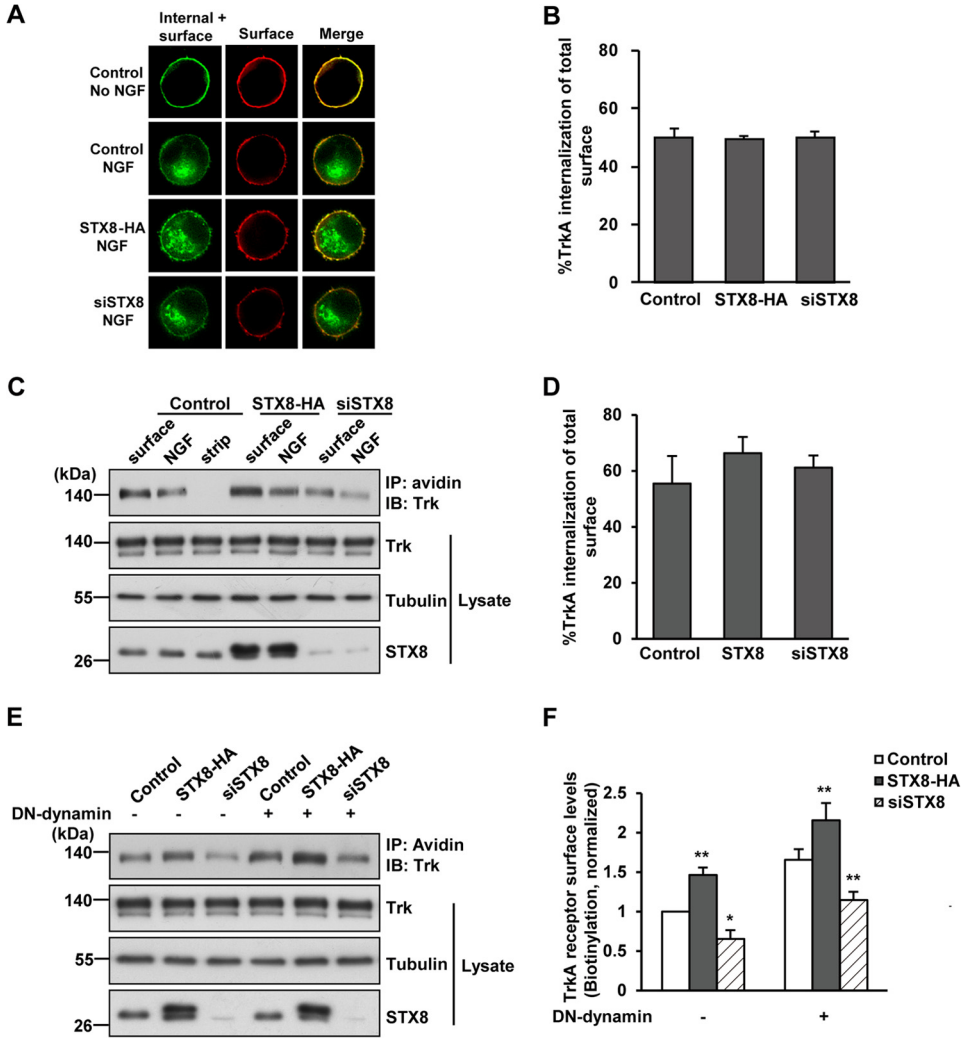

FIGURE 4. **STX8 modulates TrkA cell surface levels via the post-biosynthetic but not the endocytic pathway.** *A,* representative images from a ratiometric fluorescence assay to measure the internalization of TrkA receptor as described under "Experimental Procedures" in PC12 cells transfected with FLAG-TrkA and STX8-HA, siSTX8, or the control vector construct. The *green* color represent total Alexa Fluor-488M1-labeled FLAG-TrkA receptors, including internal and surface-remaining receptors, and the *red* pseudo-color represents the remaining FLAG-TrkA at cell surface with or without NGF incubation. *Scale bar,* 5 μm. *B,* quantification of the NGF-induced internalization of TrkA in *A* as described under "Experimental Procedures." *C,* cleavable surface biotinylation assays were performed in 615 cells to measure TrkA internalization. The lane labeled *surface* shows the cell surface TrkA levels without NGF treatment; the lane labeled *NGF* shows the endocytic TrkA, and the lane labeled *strip* shows a control for the efficiency of the stripping procedure. *IB,* immunoblot. *D,* quantification of the NGF-induced internalization of TrkA in *C*. The data are presented as internalization percentage of total surface receptors. *E,* noncleavable surface biotinylation was used to measure TrkA cell surface levels in 615 cells that were co-transfected by electroporation with a dominant-negative form of dynamin (*DN-dynamin*) to block TrkA internalization. *F,* quantification of cell surface TrkA levels in *E*. The data are shown as means ± S.E. (*, $p < 0.05$; **, $p < 0.01$ *versus* their corresponding controls, one-way ANOVA).

gested that STX8 regulates TrkA surface levels via its interaction with the TrkA CT domain.

STX8 Facilitates TrkA Surface Targeting via the Post-biosynthetic Pathway—As the surface levels of TrkA depend on insertion and endocytosis, opposite receptor trafficking processes, we next sought to determine which process STX8 regulates. We first performed a ratiometric fluorescence assay measuring the internalization of the TrkA receptor as described under "Experimental Procedures" to investigate the effect of STX8 on TrkA internalization. We found that after 15 min of NGF stimulation, ~50 ± 2% of surface TrkA was internalized, and the internalization of TrkA remained unaffected under STX8 overexpression or knockdown conditions (Fig. 4, *A* and *B*), suggesting that STX8 is not involved in TrkA internalization. To further confirm this result, a cleavable surface biotinylation assay was performed in 615 cells to measure TrkA internalization. We acquired a similar result as the ratiometric fluorescence assay that ~56 ± 9% of surface TrkA was internalized (Fig. 4, *C* and *D*), which is unaffected by STX8 expression, confirming that STX8 is not involved in TrkA internalization. Moreover, previous studies have shown that the internalization of TrkA depends on dynamin, which functions in vesicle scission during clathrin-mediated endocytosis (21). A dominant-negative form of dynamin (Dynamin-K44A, DN-dynamin) can be used to suppress TrkA internalization (22, 23). Therefore, we examined whether STX8 still regulated TrkA surface levels when TrkA internalization was blocked. By the surface biotinylation assay, we found that blocking internalization by DN-dynamin in 615 cells led to an increase in the cell surface levels of TrkA receptors, and STX8 still regulated TrkA surface levels (Fig. 4, *E* and

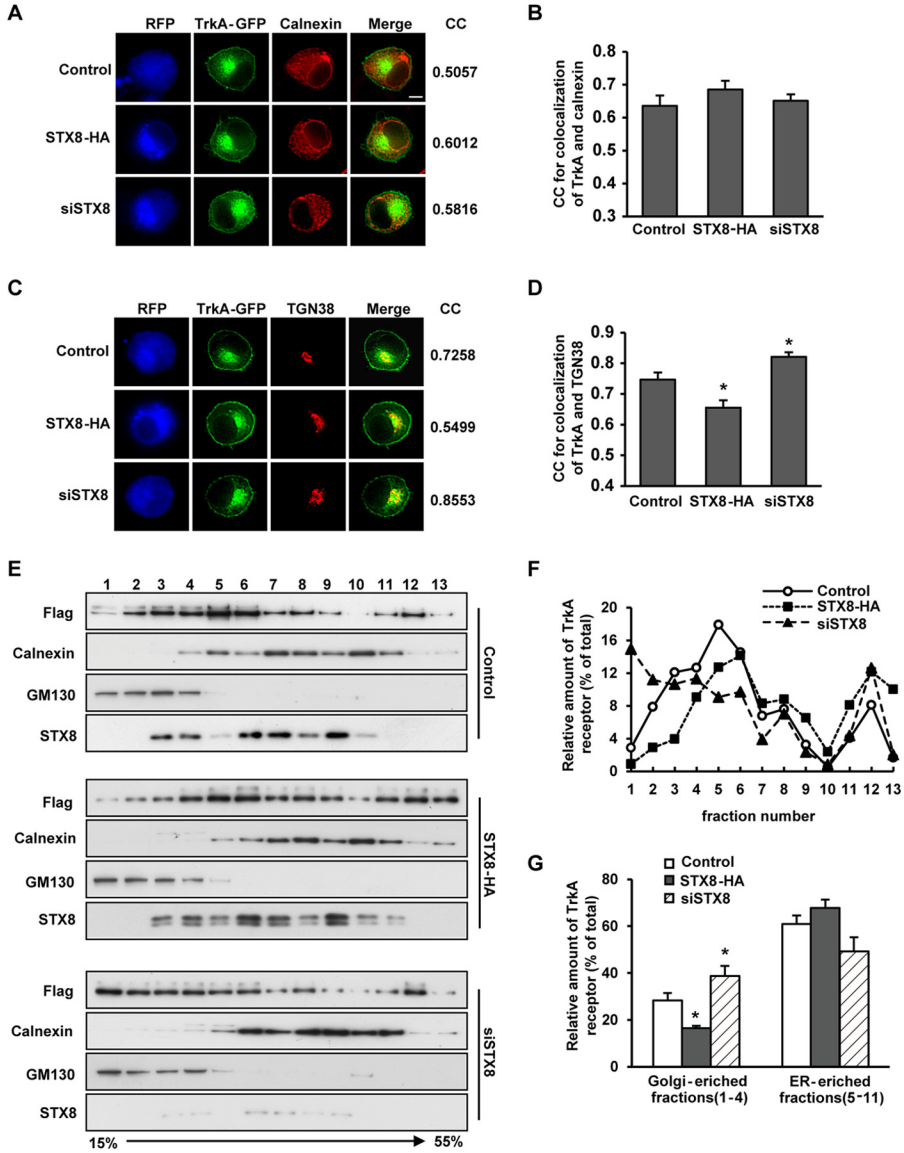

FIGURE 5. **STX8 promotes TrkA trafficking from the Golgi to the plasma membrane.** *A,* correlation analysis of the co-localization of TrkA-GFP and the ER marker calnexin in PC12 cells. PC12 cells transfected with FLAG-TrkA-GFP and STX8-RFP, pSuper-siSTX8-RFP, or the control construct pmRFP-N1 were stained with anti-calnexin antibody and Cy5-conjugated secondary antibody after permeabilization. The *blue* and *red* pseudo-colors represent RFP and calnexin, respectively. The correlation coefficients (*CC*) between TrkA and calnexin were measured using the MetaMorph correlation plot module. *Scale bar,* 5 μm. *B,* quantification of the CC in *A*. *C,* correlation analysis of the co-localization of TrkA-GFP and the trans-Golgi network marker TGN38 as described in *A*. *D,* quantification of the CC in *C*. The results are presented as the mean ± S.E. from three independent experiments. *E,* post-nuclear supernatants of PC12 cells transfected with FLAG-TrkA and STX8-HA, siSTX8, or control vector construct were fractioned on an isopycnic 15–55% (w/w) linear sucrose gradient, and equal aliquots of the final equilibrium gradient fractions (*top*, fraction 1) were immunoblotted using antibodies against GM130, calnexin and FLAG (for detecting FLAG-TrkA). *F,* quantification of TrkA immunoreactivity in the gradient fractions presented as a percentage of the total (the sum of the gradient fractions) among the three groups. *G,* quantification of the TrkA relative intensity in the Golgi- or ER-enriched fractions, presented as a percentage of the total. The data show the means of three independent experiments (*, $p < 0.05$, *versus* their corresponding controls, one-way ANOVA).

F). When TrkA internalization was blocked, the cell surface receptors were regulated only by the biosynthetic pathway. Therefore, these results suggest that STX8 modulates TrkA surface levels via the post-biosynthetic but not the endocytic pathway.

STX8 Promotes TrkA Export from the Golgi—Newly synthesized proteins destined for the plasma membrane were inserted co-translationally into the endoplasmic reticulum (ER); after their correct folding, they were transferred to the Golgi apparatus where they were modified and sorted for transport to the plasma membrane. To further investigate whether STX8 regulates TrkA ER-to-Golgi trafficking or post-Golgi sorting, we first examined whether STX8 overexpression or knockdown affected the TrkA localization in the ER or the Golgi in PC12 cells by detecting the immunofluorescence co-localization between TrkA and the ER marker calnexin or the TGN marker TGN38 (Fig. 5, *A* and *C*). The co-localization was quantified using the MetaMorph "correlation plot" module, and the values of the correlation coefficients (CC) were calculated. The theoretical range of values of the CC is −1.0 to +1.0. The value of 1.0 indicates perfectly correlated data, which only occurs if the two images are identical. A CC of −1.0 occurs only in the case of an inverse relationship in intensity between the two images. The co-localization CCs between TrkA and calnexin showed no sig-

nificant difference between the three groups (Fig. 5*B*). However, the co-localization of TrkA and TGN38 was poorer in the high STX8 expression group, although it was better in the STX8-depleted group (Fig. 5*D*). These data suggested that STX8 regulated TrkA location in Golgi apparatus.

These results were further confirmed using a biochemical approach. We performed a sucrose density gradient centrifugation assay to separate organelles in PC12 cells and used GM130 and calnexin to identify Golgi- and ER-enriched fractions, respectively (Fig. 5*E*). We observed that GM130 was present mainly in fractions 1–4, and calnexin mainly existed in fractions 5–11. By quantifying the TrkA percentage in each gradient fraction (Fig. 5*F*) and in the Golgi- or ER-enriched fractions (Fig. 5*G*), we found that there was no significant difference in TrkA levels in the ER-enriched fractions among the three groups; however, the TrkA percentage in the Golgi-enriched fraction was reduced in the STX8 overexpression group and increased in the STX8 depletion group compared with the control group (Fig. 5*G*). Therefore, these results indicate that STX8 promotes TrkA export from the Golgi apparatus and its targeting to the plasma membrane, thus increasing the TrkA surface levels. In contrast, STX8 depletion leads to the retention of TrkA in the Golgi apparatus.

STX8 Modulates NGF-induced Downstream Signaling and DRG Neuron Survival—Changes in cell surface receptor levels could lead to altered responses of the cells to the corresponding ligands. What are the functional consequences of STX8-regulated TrkA cell surface localization? To answer this question, we first examined the effect of STX8 on NGF-induced signal transduction. After serum starvation for 12 h, 615 cells were incubated with NGF (50 ng/ml) for 10 or 60 min. We observed that STX8 overexpression enhanced NGF-induced activation of the TrkA receptor and the downstream MAPK/ERK1/2 and PI3K/Akt signaling pathways by detecting the levels of phospho-TrkA, phospho-ERK1/2, and phospho-Akt; in contrast, siRNA-mediated knockdown of STX8 attenuated NGF-induced signaling (Fig. 6, *A* and *B*). These data suggest that STX8 regulates NGF-induced downstream signaling by modulating the TrkA cell surface levels.

DRG neurons depend on neurotrophin signaling for their survival. Trk receptors mediate the responses of DRG neurons to neurotrophins, and the majority of DRG neurons expresses at least one member of the Trk family. TrkA is expressed predominantly in small- and medium-sized neurons, whereas TrkB is expressed in large neurons (24). Trk expression in a particular class of DRG neurons determines the neurotrophin dependence of that class during development (25). Therefore, NGF-dependent and BDNF-dependent DRG neurons are generated. Because STX8 modulated the surface levels of TrkA but not TrkB receptors, we examined the effect of STX8 on the survival of the two types of DRG neurons. We first filtered the NGF- and BDNF-dependent cultured DRG neurons as described previously (26) and synchronously infected these neurons with lentiviruses harboring RFP, STX8-RFP, or STX8ΔTM-RFP. Apoptotic neurons were detected using TUNEL staining after the corresponding neurotrophin in the medium was switched to 1.25 ng/ml for 24 h (Fig. 6*C*). We observed that neurons in the control group showed ~66 ± 4% apoptosis upon the addition of the low concentration of neurotrophins. The percentage of apoptotic NGF-dependent neurons was markedly reduced to 50 ± 4% in the STX8-overexpressing cells (Fig. 6*D*). Concomitantly, in the STX8ΔTM-infected cells there was a significant increase (84 ± 8%) in the apoptotic NGF-dependent neurons. Conversely, STX8 had no effect on the apoptosis of BDNF-dependent DRG neurons (Fig. 6*D*). Previous studies suggested that cleaved caspase-3 plays an important role in apoptotic death of neurons induced by NGF deprivation (27), so cleaved caspase-3 was detected by Western blotting in filtered DRG neurons to confirm the result of the TUNEL staining. As shown in Fig. 6*E*, STX8 overexpression reduced the levels of cleaved caspase-3, although STX8 inhibition had the opposite effect in NGF-dependent DRG neurons but not in BDNF-dependent neurons. Together, these observations suggest that STX8 regulates NGF-induced signaling and specifically affects the survival of NGF-dependent DRG neurons.

STX8 Depletion in TrkA-positive DRG Neurons Relieves Inflammatory Pain in Vivo—The NGF-TrkA pathway appears to play a pivotal role in the generation and maintenance of several types of acute and chronic pain (28). On this basis, both the NGF and TrkA receptors are eligible targets for pain therapy (29–31). Given that STX8 could modulate TrkA cell surface trafficking and influence NGF-TrkA signaling, we sought to examine whether STX8 depletion in DRG neurons has analgesic potential in a rat inflammatory pain model.

rAAV6 has been used successfully as a vehicle to deliver genes to DRG neurons by intrathecal administration, and more than 70% of rAAV6-infected neurons were small or medium ($<700\ \mu m^2$) (32). The rAAV6-delivered gene and the TrkA receptor were co-labeled; thus, we knocked down STX8 expression in rat DRG neurons by rAAV6-mediated RNA interference. Meanwhile, rAAV8 is considered to preferentially target large diameter DRG neurons (33, 34), so we used rAAV8 as a control to infect TrkA-negative neurons. rAAV6-siSTX8-ZsGreen and rAAV8-siSTX8-GFP were intrathecally injected into the cerebrospinal fluid through the L4/5 intervertebral space. At 4 weeks post-injection, the DRG (L4 and L5) were removed from the injected rats, and by epifluorescence observation, we found that the delivery resulted in efficient transduction of the genes to DRG neurons (Fig. 7*A, panel a*). From immunohistochemical staining, we observed that ZsGreen was co-expressed with βIII-tubulin, a neuron marker (Fig. 7*A, panel d*), and the infected DRG neurons expressed TrkA receptors (Fig. 7*A, panel b*). rAAV8-infected neurons were all TrkA-negative neurons (Fig. 7*A, panel e*). The STX8 staining revealed that STX8 expression was knocked down in the infected DRG neurons (Fig. 7*A, panel c*).

The formalin test that has been widely used to study inflammatory pain (35) was carried out to detect the effect of STX8 on inflammatory pain at 4 weeks post-injection of rAAV. 50 μl of 5% formalin solution was subcutaneously injected into the plantar aspect of the right hind paw of the rats. Formalin injection resulted in the typical biphasic paw-licking response in the injected paw. The early short lasting phase (phase I, 0–10 min) is thought to result from direct activation of nociceptors, and the delayed second phase (phase II, 10–60 min) seems to result

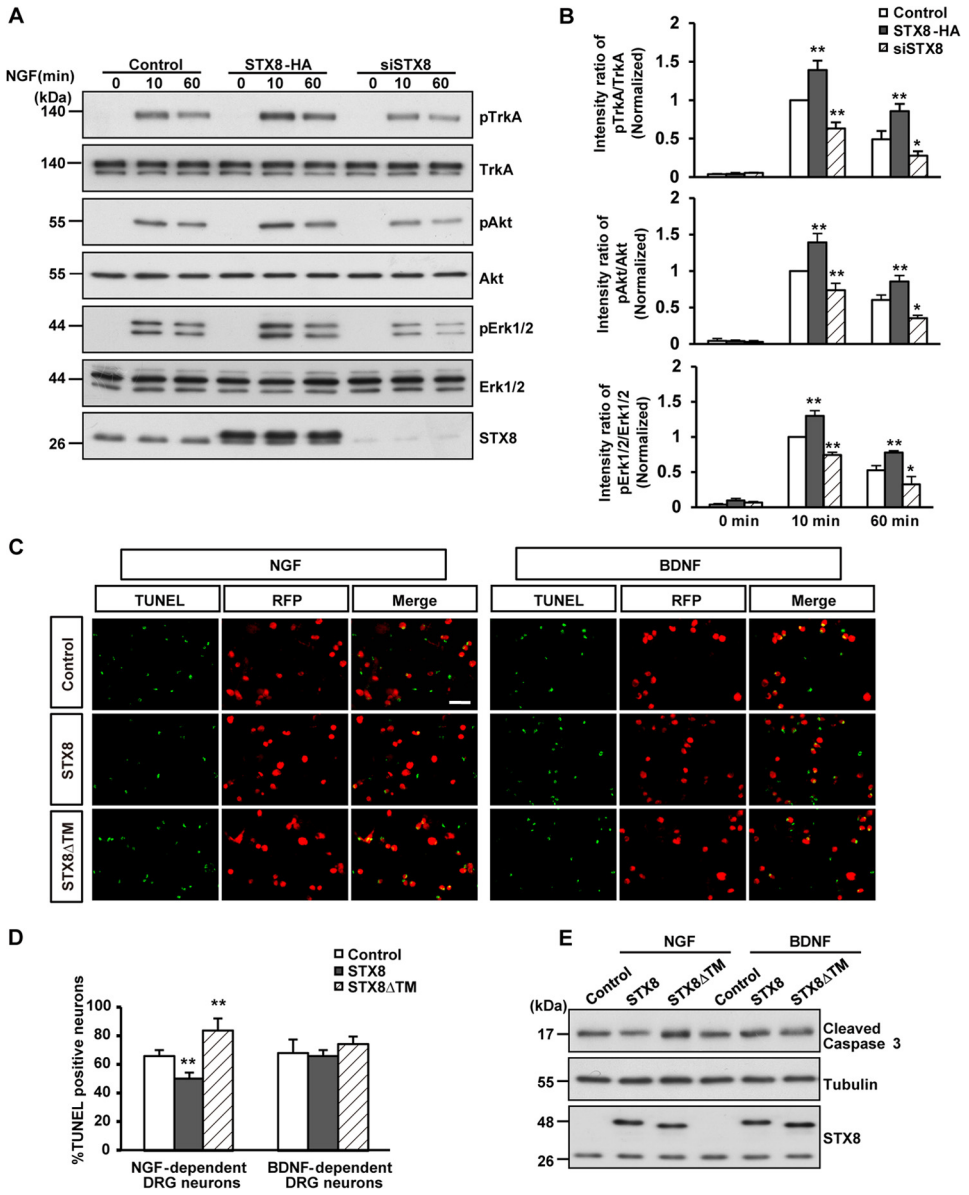

FIGURE 6. **STX8 regulates NGF-induced signal transduction and the survival of NGF-dependent DRG neurons.** *A,* 615 cells transfected with STX8-HA, siSTX8, or control vector construct by electroporation were serum-starved overnight and treated with NGF (50 ng/ml) for 10 or 60 min. Immunoblotting was used to detect the phosphorylation of TrkA, Akt, and ERK1/2. *B,* quantification of TrkA, Akt, and ERK1/2 activation by the ratios of phospho-TrkA/Akt/ERK1/2 *versus* the total corresponding protein. The data are shown as the means ± S.E. ($n = 3$, *, $p < 0.05$; **, $p < 0.01$ *versus* their corresponding controls, one-way ANOVA). *C,* DRG neurons cultured for 24 h were infected with lentiviruses expressing RFP, STX8-RFP, or STX8ΔTM-RFP in the presence of NGF (50 ng/ml) or BDNF (50 ng/ml) for 7 days. After the neurons were switched to media containing 1.25 ng/ml NGF or BDNF for 24 h, TUNEL staining was performed according to the manufacturer's instructions. *Scale bar,* 100 μm. *D,* quantification of the percentage of apoptotic neurons. The data are shown as the mean ± S.E. ($n = 3$, **, $p < 0.01$ *versus* their corresponding controls, one-way ANOVA). *E,* DRG neurons treated as in *C* were lysed and immunoblotted to detect cleaved caspase-3.

from an inflammatory response (35). The cumulative time spent in spontaneous paw-licking behavior in phases I and II was calculated. As shown in Fig. 7*B*, in phase I no significant difference in paw-licking time was observed between the STX8 deletion group and the control group, whereas in phase II, rAAV6-siSTX8-injected rats spent less time (301 ± 28 s, $n = 12$) in spontaneous pain behavior than control rats (477 ± 56 s, $n = 8$). The time course curves of paw-licking behavior in 5-min intervals showed two obvious phases in the formalin test, and in phase II, a decreased response could be observed in rAAV6-siSTX8-injected rats (Fig. 7*B*). Conversely, rAAV8-mediated STX8 silencing in TrkA-negative neurons had no effect on formalin-induced paw-licking (Fig. 7*C*), which excludes the possibility that the behavioral changes in rAAV6-injected rats were caused by STX8 knockdown in TrkA-negative neurons. These data suggest that STX8 depletion in TrkA-positive DRG neurons could induce analgesic effects in the formalin-induced inflammatory pain response.

To investigate whether the STX8 depletion decreases TrkA surface levels *in vivo* and leads to the analgesic effects, a biochemical approach was used after the formalin test. The bilateral DRGs (L4 and L5) of tested rats injected with rAAV6 were homogenized for Western blot analysis. The ipsilateral DRGs were those on the same side as the formalin injection, and the contralateral DRGs were those on the opposite side of the formalin injection, which were used as negative controls. The

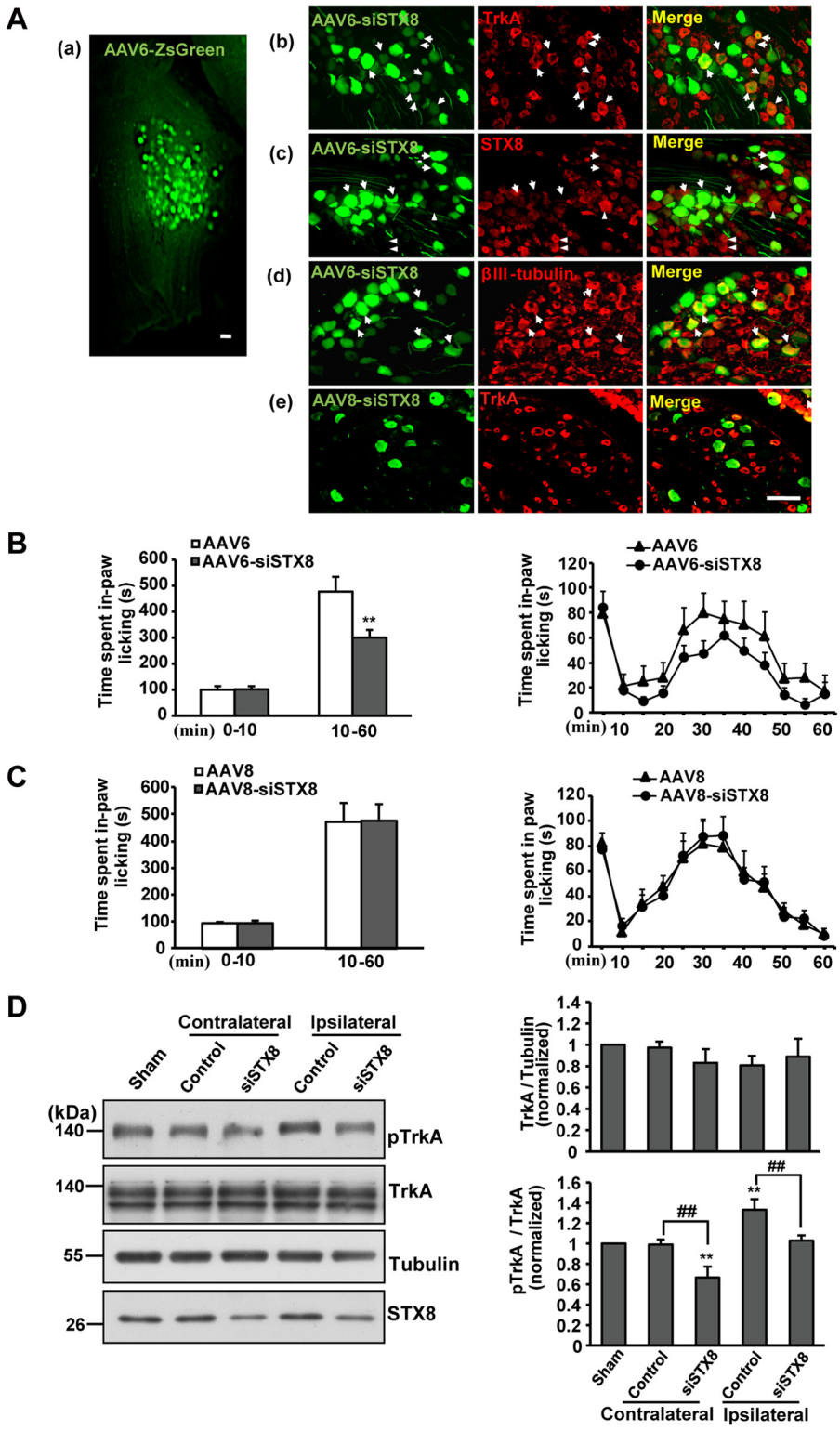

FIGURE 7. **STX8 depletion in TrkA-positive DRG neurons reduces sensitivity to formalin stimuli in rats.** *A,* rAAV transduction of the L4/5 DRG at 4 weeks after intrathecal injection. *Panel a,* macroscopic view of rat DRG injected with rAAV6 expressing ZsGreen. *Panel b,* DRG sections were processed for immunohistochemical staining. Neurons co-express ZsGreen and TrkA receptors (*arrowheads*). *Panel c, arrowheads* show the effective silencing of STX8 expression in the infected neurons, and *triangles* show normal staining in the uninfected neurons. *Panel d,* βIII-tubulin staining revealed the effective transduction of rAAV6 into DRG neurons (*arrowheads*). *Panel e,* rAAV8 infects TrkA-negative neurons. *Scale bar,* 100 μm. *B, left,* cumulative time spent performing spontaneous pain behavior in phases I and II of the formalin test in rAAV6-siSTX8-injected rats. The test evoked the typical biphasic nociceptive response as follows: phase I (0–10 min) and phase II (10–60 min) ($n = 8$–12, **, $p < 0.01$ *versus* the corresponding control group, Student's *t* test). *Right,* time course curves of spontaneous pain behavior following intraplantar injection of formalin at 5-min intervals. *C,* pain behaviors in response to the formalin test in rAAV8-siSTX8-injected rats. *D,* bilateral L4/5 DRGs of rats injected with rAAV6 were lysed after the formalin test, and Western blotting was performed to examine the expression of various proteins, including pTrkA, TrkA, and STX8. The data are shown as the means ± S.E. ($n = 5$, **, $p < 0.01$ *versus* the sham group; ##, $p < 0.01$, *versus* the corresponding controls, one-way ANOVA).

knockdown of STX8 did not influence the total TrkA levels; however, formalin injection resulted in an increase in phospho-TrkA levels on the ipsilateral side of the DRGs, which was consistent with the concept that the NGF-TrkA signal plays an important role in inflammatory pain transmission (Fig. 7*D*) (28). In the presence of inflammatory stimuli, NGF activates TrkA in surface membranes of peripheral terminals, and the NGF-TrkA complex is transported to the cell bodies of DRG neurons. It then activates transcription factors and controls downstream gene expression. Thus, phospho-TrkA levels could indirectly reflect the surface TrkA levels in DRG neurons in the inflammatory response. STX8 depletion resulted in a reduction in phospho-TrkA levels on both sides compared with their respective control groups (Fig. 7*D*). These results suggest that pain attenuation following STX8 depletion was associated with a decrease in NGF-TrkA signal activation.

DISCUSSION

A neuron's response to neurotrophins requires Trk receptors localized at the cell surface. Therefore, TrkA localization plays an important role in NGF-TrkA signaling and function; however, the underlying mechanism of TrkA surface targeting remains poorly understood. This study identified STX8 as a novel regulator of the cell surface localization of TrkA but not the TrkB receptor by facilitating TrkA Golgi-to-plasma membrane trafficking.

Our studies provide several novel insights into the regulation of TrkA cell surface levels and its physiological relevance. First, we found that STX8 is involved in modulating cell surface levels of TrkA but not TrkB receptors. An amino acid sequence analysis revealed that TrkA and TrkB are highly homologous, and the peptide sequences of the cytoplasmic domain are 67% identical (36). Because of high homology, TrkA and TrkB possess many similar characteristics; for example, they have similar signal transmission and biological functions. However, many studies have shown that TrkA and TrkB exhibit differential trafficking regulation mechanisms. For example, they are regulated differently by ubiquitination (26, 37). TrkA receptors associate with an E3 ubiquitin ligase, Nedd4-2, through a PP*X*Y motif leading to ubiquitination and subsequently degradation. In contrast, TrkB is not ubiquitinated by Nedd4-2 due to the lack of a consensus PP*X*Y motif. In addition, a previous study reported that TrkA and TrkB are transported through divergent endocytic trafficking pathways (15). TrkA receptors predominantly cycle back to the cell surface in a ligand-dependent manner, whereas TrkB is predominantly sorted to the degradative pathway. The different trafficking pathways resulted from the specific sequences in the juxtamembrane regions of the receptors. In our study, we found that STX8 associated with TrkA, but not TrkB receptors, via the TrkA CT domain and regulated TrkA post-biosynthetic trafficking. The TrkA CT domain seems to be necessary and sufficient for the interaction with and the regulation by STX8. Similarly to Nedd4, STX8 specifically regulated the survival of NGF-dependent DRG neurons (Fig. 6), which is consistent with its specific regulation of the cell surface trafficking of the TrkA receptors.

Second, we found that STX8 promotes TrkA export from the Golgi apparatus to the plasma membrane. The syntaxins, as members of the Q-SNARE subfamily, are well characterized for their roles in intracellular vesicle trafficking (10). Previous studies have shown that STX8 resides in the TGN, early endosome, and late endosome compartments (38, 39) and mainly regulates late endosome fusion with the lysosome or homotypic lysosome fusion (10). Bilan *et al.* (14) reported that STX8 overexpression reduces cell surface cystic fibrosis transmembrane conductance regulator levels. Conversely, our study found that STX8 modulates TrkA Golgi-to-plasma membrane trafficking and enhances TrkA cell surface levels. Although this process differs from the STX8-mediated classical endosomal trafficking, there are several pieces of data that support it. First, STX6 and STX10, STX8 homologues, are localized primarily in the Golgi apparatus and are involved in the transport of molecules to and from the Golgi apparatus (10, 40). For example, STX6 has been reported to regulate VEGFR2 trafficking through the Golgi apparatus en route to the plasma membrane (13). STX8 also partially localizes to the TGN, so it is possible that it functions in TGN trafficking. Second, the function of SNARE molecules in protein trafficking is complicated. The same family member could be involved in several trafficking events. For example, the Q-SNARE SNAP-25 plays critical roles not only in NMDA receptor insertion (41) but also in the internalization of kainate receptors (42). Therefore, it is possible that STX8 is involved in post-biosynthetic trafficking in addition to classical endosomal trafficking. In our study, STX8 overexpression reduced TrkA levels in the Golgi, and conversely, STX8 knockdown resulted in the accumulation of TrkA in the Golgi (Fig. 5), which indicates that STX8 promotes TrkA export from the Golgi apparatus. However, we still do not know how STX8 functions in Golgi-related trafficking and whether there is an STX8-independent mechanism involved in the process.

Finally, we found that STX8 is involved in NGF-mediated biological functions. We confirmed that STX8 modulates TrkA-mediated downstream Akt and ERK pathway activation (Fig. 6*A*). The activation of the PI3K/Akt and MAPK/ERK1/2 pathways is responsible for the NGF-TrkA survival activity (43). Thus, STX8 could modulate the survival of NGF-dependent DRG neurons. Interestingly, STX8 has no effect on the survival of BDNF-dependent DRG neurons (Fig. 6), which is consistent with our result that STX8 regulates the cell surface levels of TrkA but not TrkB receptors. The DRG play critical roles in pain sensitivity and transmission to the CNS. NGF binds a terminal surface TrkA in DRG neurons, and NGF-TrkA signaling activates transcription factors, resulting in increased synthesis of certain pain-related proteins, including transient receptor potential vanilloid 1, voltage-gated sodium and calcium channels, and bradykinin receptors (28). Because the NGF-TrkA system is functionally placed upstream of many different molecular partners in the transmission of inflammatory pain, NGF and TrkA receptors are eligible targets for pain therapy. Previous studies have proposed several antagonists of NGF-TrkA signaling as potential analgesics, such as anti-NGF and TrkA antibodies, TrkA-IgG fusion proteins, and small molecular inhibitors of TrkA (28, 31). In our study, we found that STX8 knockdown via rAAV6-siSTX8-mediated silencing in rat DRG reduced TrkA activation and appeared effective in the relief of inflammatory pain *in vivo*; the paw licking behavior

recorded in phase II in the formalin pain model was significantly reduced (Fig. 7). The analgesia resulting from STX8 depletion may be due to the reduction in TrkA receptors on the membranes of DRG peripheral terminals. Our discovery further validates TrkA as a clinically relevant target.

In conclusion, we identified STX8 as a molecular determinant of TrkA trafficking from the Golgi to the plasma membrane. This finding suggests a novel regulatory mechanism of TrkA trafficking and function, especially in TrkA-mediated pain transmission, which may help us develop new analgesic drugs that antagonize NGF function.

REFERENCES

1. Huang, E. J., and Reichardt, L. F. (2001) Neurotrophins: roles in neuronal development and function. *Annu. Rev. Neurosci.* **24,** 677–736
2. McAllister, A. K., Katz, L. C., and Lo, D. C. (1999) Neurotrophins and synaptic plasticity. *Annu. Rev. Neurosci.* **22,** 295–318
3. Sofroniew, M. V., Howe, C. L., and Mobley, W. C. (2001) Nerve growth factor signaling, neuroprotection, and neural repair. *Annu. Rev. Neurosci.* **24,** 1217–1281
4. Chao, M., Casaccia-Bonnefil, P., Carter, B., Chittka, A., Kong, H., and Yoon, S. O. (1998) Neurotrophin receptors: mediators of life and death. *Brain Res. Brain Res. Rev.* **26,** 295–301
5. Johnson, D., Lanahan, A., Buck, C. R., Sehgal, A., Morgan, C., Mercer, E., Bothwell, M., and Chao, M. (1986) Expression and structure of the human NGF receptor. *Cell* **47,** 545–554
6. Kaplan, D. R., Hempstead, B. L., Martin-Zanca, D., Chao, M. V., and Parada, L. F. (1991) The trk proto-oncogene product: a signal transducing receptor for nerve growth factor. *Science* **252,** 554–558
7. Valdez, G., Akmentin, W., Philippidou, P., Kuruvilla, R., Ginty, D. D., and Halegoua, S. (2005) Pincher-mediated macroendocytosis underlies retrograde signaling by neurotrophin receptors. *J. Neurosci.* **25,** 5236–5247
8. Wan, J., Cheung, A. Y., Fu, W. Y., Wu, C., Zhang, M., Mobley, W. C., Cheung, Z. H., and Ip, N. Y. (2008) Endophilin B1 as a novel regulator of nerve growth factor/ TrkA trafficking and neurite outgrowth. *J. Neurosci.* **28,** 9002–9012
9. Bodmer, D., Ascaño, M., and Kuruvilla, R. (2011) Isoform-specific dephosphorylation of dynamin1 by calcineurin couples neurotrophin receptor endocytosis to axonal growth. *Neuron* **70,** 1085–1099
10. Hong, W. (2005) SNAREs and traffic. *Biochim. Biophys. Acta* **1744,** 493–517
11. Teng, F. Y., Wang, Y., and Tang, B. L. (2001) The syntaxins. *Genome Biol.* **2,** REVIEWS3012
12. Gee, H. Y., Tang, B. L., Kim, K. H., and Lee, M. G. (2010) Syntaxin 16 binds to cystic fibrosis transmembrane conductance regulator and regulates its membrane trafficking in epithelial cells. *J. Biol. Chem.* **285,** 35519–35527
13. Manickam, V., Tiwari, A., Jung, J. J., Bhattacharya, R., Goel, A., Mukhopadhyay, D., and Choudhury, A. (2011) Regulation of vascular endothelial growth factor receptor 2 trafficking and angiogenesis by Golgi localized t-SNARE syntaxin 6. *Blood* **117,** 1425–1435
14. Bilan, F., Thoreau, V., Nacfer, M., Dérand, R., Norez, C., Cantereau, A., Garcia, M., Becq, F., and Kitzis, A. (2004) Syntaxin 8 impairs trafficking of cystic fibrosis transmembrane conductance regulator (CFTR) and inhibits its channel activity. *J. Cell Sci.* **117,** 1923–1935
15. Chen, Z. Y., Ieraci, A., Tanowitz, M., and Lee, F. S. (2005) A novel endocytic recycling signal distinguishes biological responses of Trk neurotrophin receptors. *Mol. Biol. Cell* **16,** 5761–5772
16. Huang, S. H., Zhao, L., Sun, Z. P., Li, X. Z., Geng, Z., Zhang, K. D., Chao, M. V., and Chen, Z. Y. (2009) Essential role of Hrs in endocytic recycling of full-length TrkB receptor but not its isoform TrkB.T1. *J. Biol. Chem.* **284,** 15126–15136
17. Saxena, S., Howe, C. L., Cosgaya, J. M., Steiner, P., Hirling, H., Chan, J. R., Weis, J., and Krüttgen, A. (2005) Differential endocytic sorting of p75NTR and TrkA in response to NGF: a role for late endosomes in TrkA trafficking. *Mol. Cell. Neurosci.* **28,** 571–587
18. Zhao, L., Sheng, A. L., Huang, S. H., Yin, Y. X., Chen, B., Li, X. Z., Zhang, Y., and Chen, Z. Y. (2009) Mechanism underlying activity-dependent insertion of TrkB into the neuronal surface. *J. Cell Sci.* **122,** 3123–3136
19. Averill, S., McMahon, S. B., Clary, D. O., Reichardt, L. F., and Priestley, J. V. (1995) Immunocytochemical localization of trkA receptors in chemically identified subgroups of adult rat sensory neurons. *Eur. J. Neurosci.* **7,** 1484–1494
20. Fang, X., Djouhri, L., McMullan, S., Berry, C., Okuse, K., Waxman, S. G., and Lawson, S. N. (2005) trkA is expressed in nociceptive neurons and influences electrophysiological properties via Nav1.8 expression in rapidly conducting nociceptors. *J. Neurosci.* **25,** 4868–4878
21. Sever, S., Damke, H., and Schmid, S. L. (2000) Garrotes, springs, ratchets, and whips: putting dynamin models to the test. *Traffic* **1,** 385–392
22. Ye, H., Kuruvilla, R., Zweifel, L. S., and Ginty, D. D. (2003) Evidence in support of signaling endosome-based retrograde survival of sympathetic neurons. *Neuron* **39,** 57–68
23. Zhang, Y., Wang, Y. G., Zhang, Q., Liu, X. J., Liu, X., Jiao, L., Zhu, W., Zhang, Z. H., Zhao, X. L., and He, C. (2009) Interaction of Mint2 with TrkA is involved in regulation of nerve growth factor-induced neurite outgrowth. *J. Biol. Chem.* **284,** 12469–12479
24. Mu, X., Silos-Santiago, I., Carroll, S. L., and Snider, W. D. (1993) Neurotrophin receptor genes are expressed in distinct patterns in developing dorsal root ganglia. *J. Neurosci.* **13,** 4029–4041
25. White, F. A., Silos-Santiago, I., Molliver, D. C., Nishimura, M., Phillips, H., Barbacid, M., and Snider, W. D. (1996) Synchronous onset of NGF and TrkA survival dependence in developing dorsal root ganglia. *J. Neurosci.* **16,** 4662–4672
26. Yu, T., Calvo, L., Anta, B., López-Benito, S., Southon, E., Chao, M. V., Tessarollo, L., and Arévalo, J. C. (2011) Regulation of trafficking of activated TrkA is critical for NGF-mediated functions. *Traffic* **12,** 521–534
27. Wright, K. M., Vaughn, A. E., and Deshmukh, M. (2007) Apoptosome dependent caspase-3 activation pathway is non-redundant and necessary for apoptosis in sympathetic neurons. *Cell Death Differ.* **14,** 625–633
28. Mantyh, P. W., Koltzenburg, M., Mendell, L. M., Tive, L., and Shelton, D. L. (2011) Antagonism of nerve growth factor-TrkA signaling and the relief of pain. *Anesthesiology* **115,** 189–204
29. Ma, W.-Y., Murata, E., Ueda, K., Kuroda, Y., Cao, M.-H., Abe, M., Shigemi, K., and Hirose, M. (2010) A synthetic cell-penetrating peptide antagonizing TrkA function suppresses neuropathic pain in mice. *J. Pharmacol. Sci.* **114,** 79–84
30. Watson, J. J. (2006) TrkAd5: A novel therapeutic agent for treatment of inflammatory pain and asthma. *J. Pharmacol. Exp. Ther.* **316,** 1122–1129
31. Ugolini, G., Marinelli, S., Covaceuszach, S., Cattaneo, A., and Pavone, F. (2007) The function neutralizing anti-TrkA antibody MNAC13 reduces inflammatory and neuropathic pain. *Proc. Natl. Acad. Sci. U.S.A.* **104,** 2985–2990
32. Towne, C., Pertin, M., Beggah, A. T., Aebischer, P., and Decosterd, I. (2009) Recombinant adeno-associated virus serotype 6 (rAAV2/6)-mediated gene transfer to nociceptive neurons through different routes of delivery. *Mol. Pain* **5,** 52
33. Jacques, S. J., Ahmed, Z., Forbes, A., Douglas, M. R., Vigenswara, V., Berry, M., and Logan, A. (2012) AAV8(gfp) preferentially targets large diameter dorsal root ganglion neurones after both intra-dorsal root ganglion and intrathecal injection. *Mol. Cell. Neurosci.* **49,** 464–474
34. Vulchanova, L., Schuster, D. J., Belur, L. R., Riedl, M. S., Podetz-Pedersen, K. M., Kitto, K. F., Wilcox, G. L., McIvor, R. S., and Fairbanks, C. A. (2010) Differential adeno-associated virus mediated gene transfer to sensory neurons following intrathecal delivery by direct lumbar puncture. *Mol. Pain* **6,** 31
35. Tjølsen, A., Berge, O. G., Hunskaar, S., Rosland, J. H., and Hole, K. (1992) The formalin test: an evaluation of the method. *Pain* **51,** 5–17
36. Nakagawara, A., Liu, X. G., Ikegaki, N., White, P. S., Yamashiro, D. J., Nycum, L. M., Biegel, J. A., and Brodeur, G. M. (1995) Cloning and chromosomal localization of the human TRK-B tyrosine kinase receptor gene (NTRK2). *Genomics* **25,** 538–546
37. Arévalo, J. C., Waite, J., Rajagopal, R., Beyna, M., Chen, Z. Y., Lee, F. S., and Chao, M. V. (2006) Cell survival through Trk neurotrophin receptors is differentially regulated by ubiquitination. *Neuron* **50,** 549–559
38. Prekeris, R., Yang, B., Oorschot, V., Klumperman, J., and Scheller, R. H.

(1999) Differential roles of syntaxin 7 and syntaxin 8 in endosomal trafficking. *Mol. Biol. Cell* **10,** 3891–3908
39. Subramaniam, V. N., Loh, E., Horstmann, H., Habermann, A., Xu, Y., Coe, J., Griffiths, G., and Hong, W. (2000) Preferential association of syntaxin 8 with the early endosome. *J. Cell Sci.* **113,** 997–1008
40. Mallard, F., Tang, B. L., Galli, T., Tenza, D., Saint-Pol, A., Yue, X., Antony, C., Hong, W., Goud, B., and Johannes, L. (2002) Early/recycling endosomes-to-TGN transport involves two SNARE complexes and a Rab6 isoform. *J. Cell Biol.* **156,** 653–664
41. Lau, C. G., Takayasu, Y., Rodenas-Ruano, A., Paternain, A. V., Lerma, J., Bennett, M. V., and Zukin, R. S. (2010) SNAP-25 is a target of protein kinase C phosphorylation critical to NMDA receptor trafficking. *J. Neurosci.* **30,** 242–254
42. Selak, S., Paternain, A. V., Aller, M. I., Aller, I. M., Picó, E., Rivera, R., and Lerma, J. (2009) A role for SNAP25 in internalization of kainate receptors and synaptic plasticity. *Neuron* **63,** 357–371
43. Ulrich, E., Duwel, A., Kauffmann-Zeh, A., Gilbert, C., Lyon, D., Rudkin, B., Evan, G., and Martin-Zanca, D. (1998) Specific TrkA survival signals interfere with different apoptotic pathways. *Oncogene* **16,** 825–832